

The UV Galaxy Luminosity Function in the Local Universe from GALEX Data

Ted K. Wyder¹, Marie A. Treyer^{1,2}, Bruno Milliard², David Schiminovich^{1,3}, Stéphane Arnouts², Tamás Budavári⁴, Tom A. Barlow¹, Luciana Bianchi⁵, Yong-Ik Byun⁶, José Donas², Karl Forster¹, Peter G. Friedman¹, Timothy M. Heckman⁴, Patrick N. Jelinsky⁷, Young-Wook Lee⁶, Barry F. Madore⁸, Roger F. Malina², D. Christopher Martin¹, Patrick Morrissey¹, Susan G. Neff⁹, R. Michael Rich¹⁰, Oswald H. W. Siegmund⁷, Todd Small¹,
Alex S. Szalay⁴, and Barry Y. Welsh⁷

Received 2004 May 5; accepted _____

¹California Institute of Technology, MC 405-47, 1200 East California Boulevard, Pasadena, CA 91125; wyder@srl.caltech.edu

²Laboratoire d’Astrophysique de Marseille, BP 8, Traverse du Siphon, 13376 Marseille Cedex 12, France

³Department of Astronomy, Columbia University, MC2457, 550 W. 120 St., New York, NY, 10027

⁴Department of Physics and Astronomy, The Johns Hopkins University, Homewood Campus, Baltimore, MD 21218

⁵Center for Astrophysical Sciences, The Johns Hopkins University, 3400 N. Charles St., Baltimore, MD 21218

⁶Center for Space Astrophysics, Yonsei University, Seoul 120-749, Korea

⁷Space Sciences Laboratory, University of California at Berkeley, 601 Campbell Hall, Berkeley, CA 94720

⁸Observatories of the Carnegie Institution of Washington, 813 Santa Barbara St., Pasadena, CA 91101

⁹Laboratory for Astronomy and Solar Physics, NASA Goddard Space Flight Center, Greenbelt, MD 20771

¹⁰Department of Physics and Astronomy, University of California, Los Angeles, CA 90095

ABSTRACT

We present the results of a determination of the galaxy luminosity function at ultraviolet wavelengths at redshifts of $z = 0.0 - 0.1$ from GALEX data. We determined the luminosity function in the GALEX FUV and NUV bands from a sample of galaxies with UV magnitudes between 17 and 20 that are drawn from a total of 56.73 deg^2 of GALEX fields overlapping the b_j -selected 2dF Galaxy Redshift Survey. The resulting luminosity functions are fainter than previous UV estimates and result in total UV luminosity densities of $10^{25.55 \pm 0.12} \text{ ergs s}^{-1} \text{ Hz}^{-1} \text{ Mpc}^{-3}$ and $10^{25.72 \pm 0.12} \text{ ergs s}^{-1} \text{ Hz}^{-1} \text{ Mpc}^{-3}$ at 1530\AA and 2310\AA , respectively. This corresponds to a local star formation rate density in agreement with previous estimates made with $\text{H}\alpha$ -selected data for reasonable assumptions about the UV extinction.

Subject headings: surveys – galaxies: luminosity function – ultraviolet: galaxies

1. Introduction

In the past few years determinations of the star formation history of the universe have allowed us to begin to understand quantitatively when and how the stars in the universe were formed. Measurements of the rest-frame ultraviolet luminosities of galaxies have been particularly useful in this endeavor. In the very local universe, there is a relative lack of systematic surveys of galaxies in the UV. Before the launch of GALEX, the most comprehensive survey of galaxies in the local universe was from the FOCA experiment (Milliard et al. 1992), a balloon-borne telescope that made measurements in a single band centered at 2000\AA . Based upon FOCA observations of a total of $\sim 2.2\text{ deg}^2$, Treyer et al. (1998) and Sullivan et al. (2000) measured the first UV luminosity function (LF) for a sample of 273 galaxies with spectroscopic redshifts at $\bar{z} = 0.15$. Their LF has a steep faint end slope and a total UV luminosity density, and corresponding star formation rate density, larger than most previous estimates. This higher local UV luminosity density in conjunction with measurements at larger distances lead Wilson et al. (2002) to infer a luminosity density evolution proportional to $(1+z)^{1.7\pm 1.0}$, a trend shallower than had been estimated previously from the CFRS sample (Lilly et al. 1996).

In this letter we present the first results regarding the UV LF based upon measurements from the *Galaxy Evolution Explorer* (GALEX) in conjunction with redshifts from the 2dF Galaxy Redshift Survey (2dFGRS) (Colless et al. 2001). The new GALEX data allow us to expand upon the previous FOCA results using a much larger sample drawn from an area of 56.73 deg^2 although to a shallower limiting magnitude of $m_{UV} = 20$. Throughout this paper, we assume $H_0 = 70\text{ km s}^{-1}\text{ Mpc}^{-1}$, $\Omega_M = 0.3$ and $\Omega_\Lambda = 0.7$.

2. Data

The data analyzed in this paper consist of 133 GALEX All-Sky Survey (AIS) pointings that overlap the 2dF Galaxy Redshift Survey in the South Galactic Pole region. The GALEX field-of-view is circular with diameter of 1.2° and each pointing is imaged simultaneously in both the FUV and NUV bands with effective wavelengths of 1530\AA and 2310\AA , respectively. The median exposure time for the fields is 105 seconds, allowing us to reach a S/N ratio of ~ 5 for $FUV \approx 20.0$ and $NUV \approx 20.5$. See Martin et al. (2004) and Morissey et al. (2004) for details regarding the GALEX instruments and mission.

Sources were detected and measured from the GALEX images using the program SExtractor (Bertin & Arnouts 1996). As the NUV images are substantially deeper than the FUV, we used the NUV images for detection and measured the FUV flux in the same aperture as for the NUV. The fields analyzed here were processed using a larger SExtractor deblending parameter DEBLEND_MINCONT as the standard GALEX pipeline processing tends to break apart well-resolved galaxies into more than one source. We elected to use the MAG_AUTO magnitudes measured by SExtractor through an elliptical aperture whose semi-major axis is scaled to 2.5 times the first moment of the object’s radial profile, as first suggested by Kron (1980). All of the apparent magnitudes were corrected for foreground extinction using the Schlegel et al. (1998) reddening maps and assuming the extinction law of Cardelli et al. (1989). The ratio of the extinction in the GALEX bands to the reddening $E(B - V)$ was calculated by averaging the extinction law over each GALEX bandpass, resulting in $A_{FUV}/E(B - V) = 8.376$ and $A_{NUV}/E(B - V) = 8.741$. The median extinction correction for the galaxies in our South Galactic Pole sample is 0.15 mag in both bands, with the corrections ranging from 0.1 to 0.3 mag.

The GALEX catalogs were matched with the 2dFGRS input catalog using a search radius of $6''$. To remove any overlap between adjacent pointings, we only included sources

detected within the inner 0.45° of each field. In addition, sources likely contaminated by artifacts from bright stars, with 2dF redshift quality flag less than three or with effective exposure times less than 60 sec were removed. Finally, we excluded GALEX sources in regions where the 2dF redshift completeness was less than 80%. After applying all of these cuts to each band, the total area on the sky of GALEX-2dF overlap is 56.73 deg^2 .

The GALEX resolution of $6 - 7''$ (FWHM) (Morrissey et al. 2004) is not sufficient to accurately separate stars and galaxies. Furthermore, the 2dFGRS input catalog available from the 2dFGRS web page¹ only includes galaxies brighter than $b_j = 19.45$ and does not include stars. In order to assess the total completeness of our 2dF-GALEX matched sample, we normalized our results to the total galaxy number counts determined by Xu et al. (2004) based primarily upon 22.64 deg^2 of GALEX Medium Imaging Survey data overlapping the Sloan Digital Sky Survey (SDSS) Data Release 1 (Abazajian et al. 2003). As the SDSS data include stars and galaxies and reach fainter magnitudes, they result in a more accurate determination of the galaxy number counts in the UV. If we assume that the average galaxy number counts in the SDSS North Galactic Pole fields are the same as in the GALEX-2dF overlap, then the redshift completeness of the 2dF matched catalog is given by the number counts of galaxies with redshifts from 2dF divided by the total galaxy number counts from the SDSS overlap. This ratio is shown in Figure 1.

The completeness turns over at 20th mag because the redshift sample becomes incomplete for galaxies with blue ($FUV - b_j$) or ($NUV - b_j$) colors. We have limited our LF determination in each band to galaxies brighter than this limit. To avoid problems with photometry of large bright galaxies, we also imposed a bright magnitude limit of 17. The average completeness weighted by the number counts in the range $17 - 20 \text{ mag}$ is 92% in the FUV and 79% in the NUV. For objects with magnitudes brighter than 20.0 in either

¹<http://www.mso.anu.edu/2dFGRS/>

band, we visually inspected all of the 2dF spectra and removed a total of 27 objects with very broad emission lines indicating that the objects are most likely some sort of AGN. The redshift distributions for the FUV and NUV samples are shown in Figure 2.

We further restricted our sample to those galaxies with redshifts $z < 0.1$ to insure that our sample is not sensitive to evolution. The average redshifts are 0.055 and 0.058 in the FUV and NUV, respectively. After applying all of the cuts mentioned in this section, a total of 896 galaxies in the FUV and 1124 galaxies in the NUV remained. The luminosity functions for the objects with $z > 0.1$ are presented in Treyer et al. (2004).

3. Luminosity Functions

Using the FUV, NUV and b_j magnitudes, we assigned a best-fit spectral type to each galaxy using a representative subset of the SEDs from Bruzual & Charlot (2003) and determined the K-correction needed to transform the observed UV magnitudes to rest-frame measurements at $z = 0$. The K-corrections are in general quite small ($\lesssim 0.2$).

We determined the LF $\Phi(M)$ and its error $\sigma(\Phi(M))$ in each band using the V_{max} method (Felten 1976):

$$\Phi(M) = \sum f(m)/V_{max} \quad (1)$$

$$\sigma(\Phi(M)) = \left(\sum f^2(m)/V_{max}^2 \right)^{1/2} \quad (2)$$

where $f(m)$ is the inverse of the redshift completeness as estimated in §2 above and V_{max} is the maximum co-moving volume within which each galaxy could have been observed given the bright and faint limiting magnitudes of our sample and its best-fit SED. The resulting LFs are shown in Figure 3.

By minimizing χ^2 , we fit the V_{max} LF points in each band with a Schechter function (Schechter 1976): $\Phi(L)dL = \phi^*(L/L^*)^\alpha e^{-L/L^*} dL/L^*$ where ϕ^* , M^* and α were free

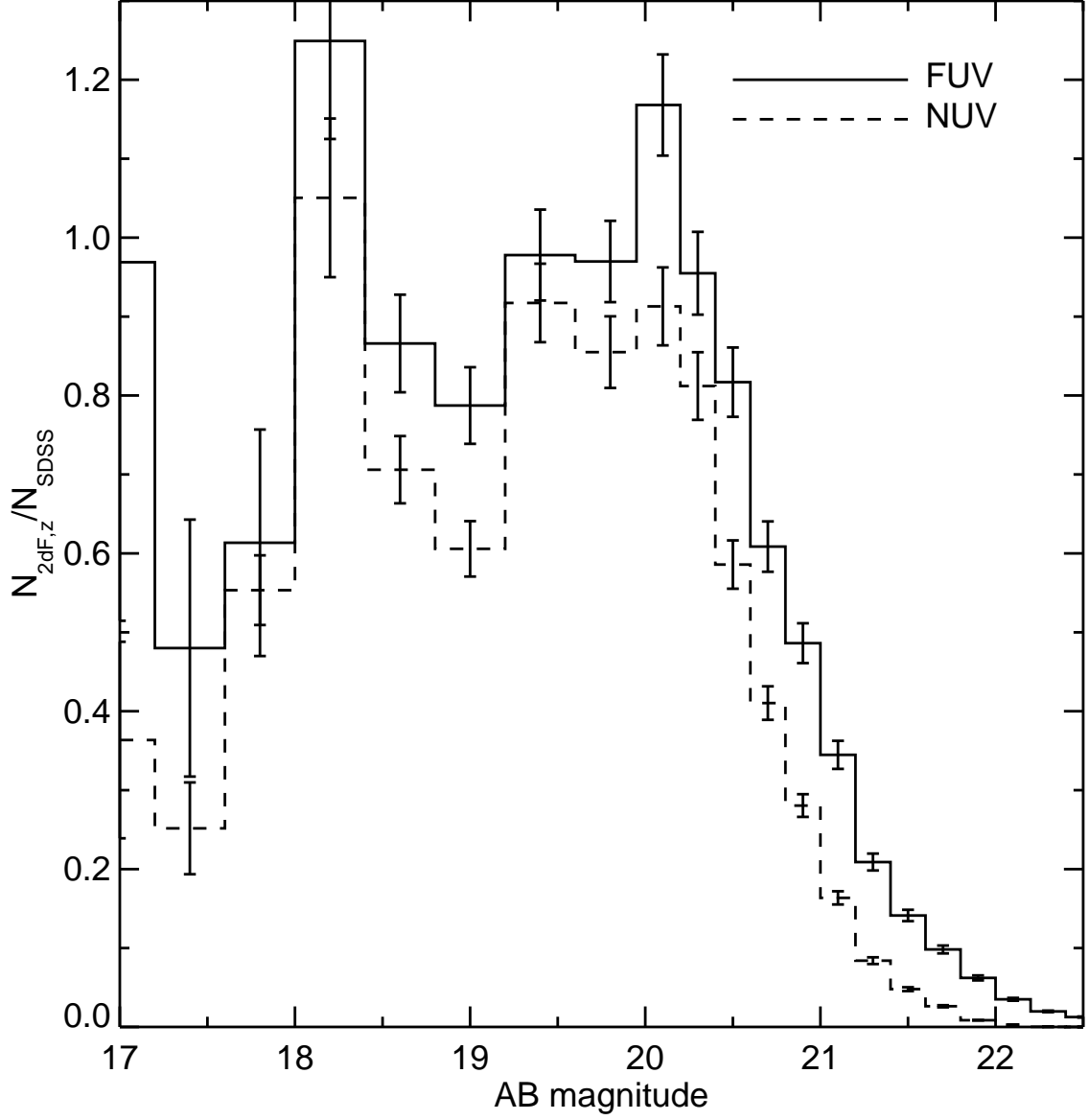


Fig. 1.— Completeness of the GALEX-2dF redshift sample defined as the ratio of the number counts of galaxies with 2dF redshifts to the number counts of galaxies as derived from GALEX observations that overlap the SDSS survey (Xu et al. 2004). The solid and dashed lines indicate the FUV and NUV redshift completeness, respectively.

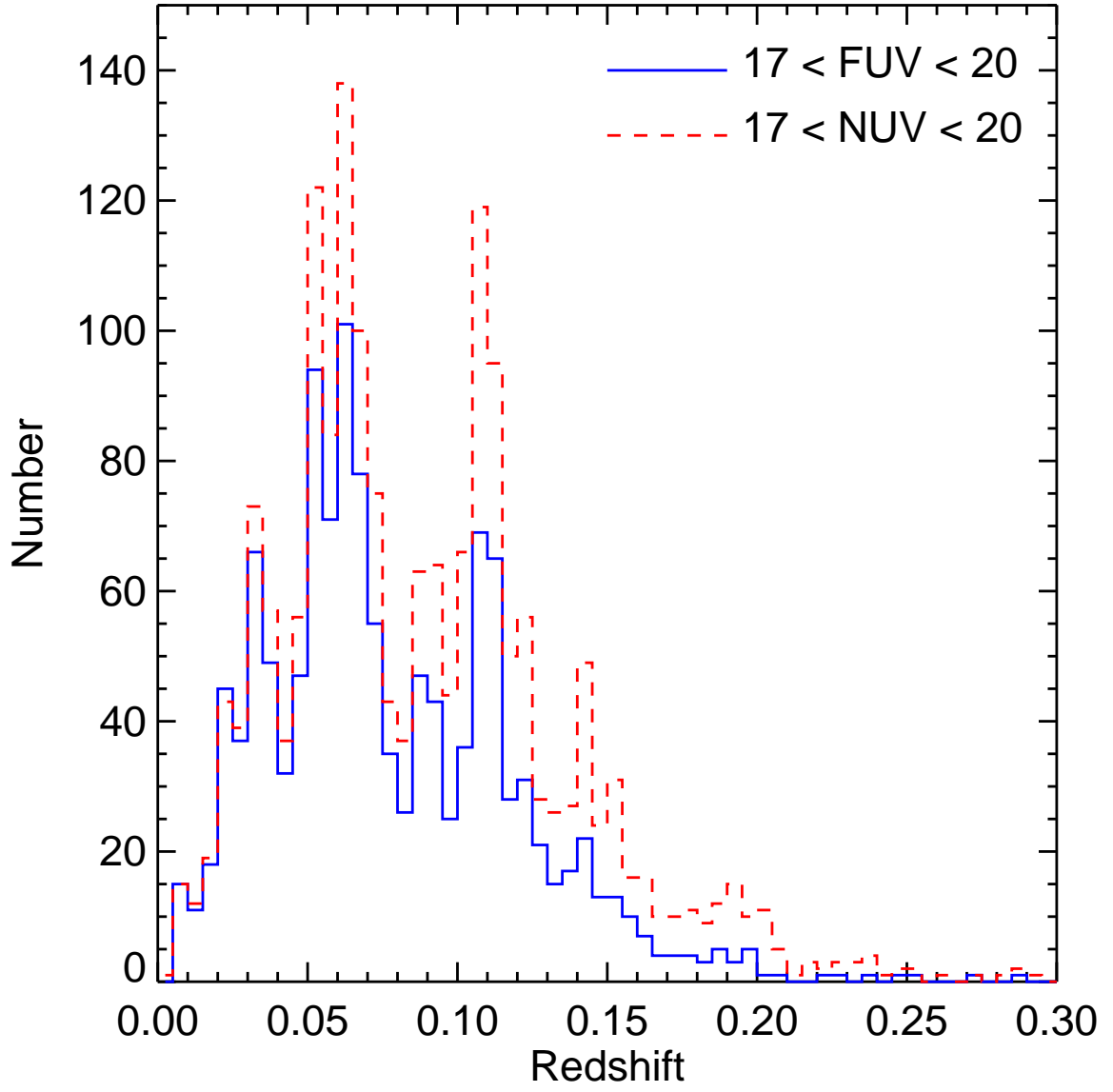


Fig. 2.— The redshift distributions of the FUV and NUV selected samples (blue solid and red dashed lines, respectively) in the range $17 \leq m_{uv} \leq 20$.

parameters. The best fit parameters and their errors, calculated using the range of solutions within 1.0 of the minimum χ^2 , are listed in Table 1 along with the best-fit LF from Sullivan et al. (2000) converted to the AB magnitude system and to $H_0 = 70$. The errors in α and M^* are highly correlated and the inset of Figure 3 shows the 1σ error contours projected into the $M^* - \alpha$ plane. Since the V_{max} method can be biased in the presence of clustering, we also computed the best-fit Schechter parameters using the maximum likelihood STY method (Sandage et al. 1979). The resulting STY values are listed in Table 1 and are also plotted in the inset of Figure 3. The STY values lie just inside and outside of the 1σ V_{max} error ellipses in the FUV and NUV, respectively. We adopt the V_{max} results in the discussion below.

4. Discussion

As can be seen in Figure 3, there are significant differences between the results presented here and those from Sullivan et al. (2000). The GALEX results have a fainter M^* in both bands and have a shallower faint end slope. The FOCA passband is centered at 2015Å with FWHM of 188Å and thus one would expect the FOCA results to lie in between the GALEX FUV and NUV data. However, the FOCA sample is truly an UV-selected sample while that presented here relies upon the b_j -selected 2dFGRS. This selection could introduce a bias in our results if the galaxies for which we do not have redshifts have a different redshift distribution than the galaxies which are included in our sample. On the other hand, it is now well established that the UV luminosity density increases with redshift (e.g. Somerville et al. 2001) and part of the difference is likely a real effect (Treyer et al. 2004). However, the difference of ~ 0.9 mag between the FOCA and NUV values for M^* would require evolution much larger than determined from other surveys as well as GALEX data at higher redshifts (Arnouts et al. 2004; Schiminovich et al. 2004). A preliminary

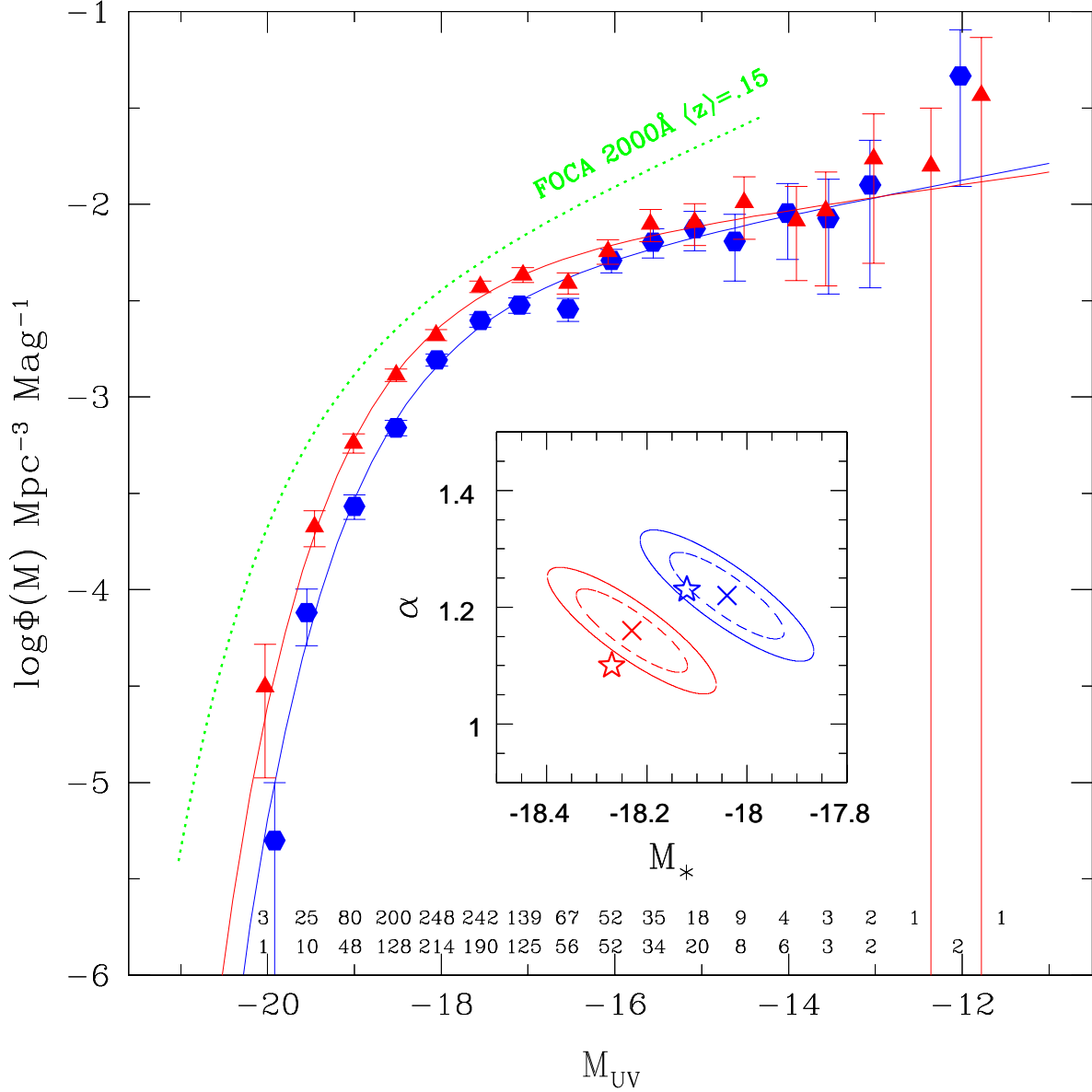


Fig. 3.— The FUV (blue circles) and NUV (red triangles) LFs for $z < 0.1$. The solid lines are the Schechter function fits with best-fit parameters from Table 1. The dotted green line shows the LF measured at 2000 Å from FOCA data by Sullivan et al. (2000) over the range of absolute magnitudes explored in that study. The inset plots the 1σ error contours of the Schechter function fits projected into the $M^* - \alpha$ plane for the FUV (blue) and NUV (red). The dashed contour shows values with $\chi^2 - \chi_{min}^2 = 1.0$ while the solid contour delineates $\chi^2 - \chi_{min}^2 = 2.3$ which corresponds to the joint 1σ uncertainty on M^* and α . The red and blue stars indicate the best-fitting values of M^* and α obtained from the STY method.

Table 1. Schechter Function Parameters

band	z	V_{max} method				STY method	
		M^*	α	$\log \phi^*$ (Mpc $^{-3}$)	$\log \rho_L$ (ergs s $^{-1}$ Hz $^{-1}$ Mpc $^{-3}$)	M^*	α
FUV	0 – 0.1	-18.04 ± 0.11	-1.22 ± 0.07	-2.37 ± 0.06	25.55 ± 0.12	-18.12	-1.23
NUV	0 – 0.1	-18.23 ± 0.11	-1.16 ± 0.07	-2.26 ± 0.06	25.72 ± 0.12	-18.27	-1.10
FOCA	0.15	-19.10 ± 0.13	-1.51 ± 0.10	-2.48 ± 0.11	26.06 ± 0.15

comparison of the GALEX and FOCA photometry in a couple of overlapping fields indicates that the FOCA magnitudes are on average brighter with the difference becoming larger for fainter sources. It appears likely these offsets and non-linearities in the FOCA photometry account for a major part of the difference between the FOCA and GALEX LFs with the remainder likely due to a combination of galaxy evolution and the FOCA sample selection.

In Table 1 we also list the total luminosity density calculated from the best-fit Schechter parameters as $\rho_L = \int_0^\infty L\Phi(L)dL = \phi^*L^*\Gamma(\alpha + 2)$. The statistical errors in $\log \rho_L$ that take into account the covariance between the three Schechter function parameters are 0.02 in each band. In addition to this error, the uncertainty in the GALEX photometric zeropoint is $\approx 10\%$ in both bands, corresponding to an uncertainty in $\log \rho_L$ of 0.04. A potentially larger source of error is that due to large scale structure. The variation in the number density of galaxies \bar{n} in a contiguous volume V is given approximately by $\delta\bar{n}/\bar{n} \approx (J_3/V)^{1/2}$ (Davis & Huchra 1982) where J_3 is an integral over the galaxy 2-point correlation function and has a value of $\sim 10^4 \text{ Mpc}^3$ for a correlation function of the form $\xi(r) = (r/r_0)^{-\gamma}$ with $r_0 = 7.21\text{Mpc}$ and $\gamma = 1.67$ (Hawkins et al. 2003). The galaxy number counts from Xu et al. (2004) used to set the normalization of our LFs were derived from approximately 22.64 deg^2 . For $z < 0.1$, the corresponding rms variation in the number density would be $\delta n/n \approx 0.24$, or an uncertainty in $\delta \log \rho_L \approx 0.11$. Since UV-selected, star-forming galaxies are likely less clustered than optically-selected samples, this value is really an upper limit. Adding these uncertainties due to large scale structure and calibration in quadrature to the statistical errors results in a total uncertainty of $\delta \log \rho_L \approx 0.12$ in both bands.

The spectral slope β , defined as $f_\lambda \propto \lambda^\beta$ with f_λ in units of $\text{ergs s}^{-1} \text{ \AA}^{-1} \text{ Mpc}^{-3}$, corresponding to our two luminosity density measurements is $\beta \approx -1.1$. This is slightly bluer than the slope of $\beta = -0.9$ determined by Cowie et al. (1999) at $z = 0.7 - 1.3$ from measurements at longer rest frame wavelengths spanning 1700\AA to 2750\AA .

The FUV luminosity density can be used to estimate the star formation rate (SFR) density in the local universe. For a constant star formation history and a Salpeter IMF, the SFR is related to the UV luminosity L_ν (in the range 1500 – 2800Å) by $\text{SFR} (\text{M}_\odot \text{ yr}^{-1}) = 1.4 \times 10^{-28} L_\nu (\text{ergs s}^{-1} \text{ Hz}^{-1})$ (Kennicutt 1998). For the FUV luminosity density in Table 1, we obtain $\log (\text{SFR}_{\text{FUV}})(\text{M}_\odot \text{ yr}^{-1} \text{ Mpc}^{-3}) = -2.30 \pm 0.12$ with no extinction correction. For comparison, the extinction-corrected $\text{H}\alpha$ LF at $z \lesssim 0.045$ from Gallego et al. (1995) shifted to our assumed Hubble constant corresponds to $\log (\text{SFR}_{\text{H}\alpha}) = -1.86 \pm 0.04$ using the $\text{H}\alpha$ to SFR conversion from Kennicutt (1998). Based upon $\text{H}\alpha$ imaging of a subsample of the galaxies used by Gallego et al. (1995), Pérez-González et al. (2003) argued that the local $\text{H}\alpha$ luminosity density is $\sim 60\%$ higher due to uncertainties in the aperture corrections applied to the spectroscopic data and corresponds to $\log (\text{SFR}_{\text{H}\alpha}) = -1.6 \pm 0.2$. Bringing the FUV SFR into agreement with this result would require an extinction of $A_{\text{FUV}} \simeq 1.8$.

An average extinction of $A_{\text{FUV}} \simeq 1.8$ is consistent with a simple estimate made using the observed ($\text{FUV} - \text{NUV}$) colors. While there is a well-defined relationship between the UV extinction and the spectral slope for starburst galaxies, more quiescent galaxies tend to have less extinction for a given UV slope than would be inferred from nearby starbursts (Bell 2002). In particular Kong et al. (2004) used the population synthesis models of Bruzual & Charlot (2003) along with the prescription described in Charlot & Fall (2000) for determining how starlight is absorbed by dust in galaxies to show that the smaller extinction in non-starburst galaxies can be explained by variations in the galaxies’ star formation histories. Based upon a set of Monte Carlo realizations of these models spanning a range of extinctions, ages and star formation histories, Kong et al. (2004) were able to approximate the dependence of the FUV extinction on the UV spectral slope β with the following formula: $A_{\text{FUV}} = 3.87 + 1.87(\beta + 0.40 \log b)$ where the variable b parametrizes the star formation history and is defined as the ratio of current to the past average star formation

rate. Assuming a constant star formation history ($b = 1$), an extinction of $A_{FUV} = 1.8$ is obtained for a spectral slope $\beta = -1.1$, a value consistent with that measured from the FUV and NUV luminosity densities. On the other hand, the average $(FUV - NUV)$ color of our FUV-selected sample is 0.14, corresponding to a spectral slope of $\beta = -1.67$. For this β and $b = 1$, the Kong et al. (2004) formula results in $A_{FUV} = 0.7$ mag. This extinction is similar to the results of Buat et al. (2004) who found that the average extinction for a local NUV-selected sample is $A_{FUV} \simeq 1$ mag based upon the FIR to UV flux ratio. If an extinction of $A_{FUV} \simeq 1$ is more appropriate for the UV-selected sample presented here, then the UV-based star formation rate density would be $\log(\text{SFR}_{\text{FUV}}) = -1.9 \pm 0.1$, a value lower than that from $\text{H}\alpha$ although still consistent to within the errors. In reality the extinction is likely a function of absolute magnitude and future GALEX papers will address in more detail correcting UV fluxes for extinction in a more rigorous way.

In the near future we will continue our investigation of the UV luminosity function in the local universe using GALEX AIS data covering $\sim 1000 \text{ deg}^2$ of the SDSS. In addition to expanding our sample to include more galaxies, we will use the SDSS photometry and spectroscopy to explore the dependence of UV luminosity on other galaxy characteristics, such as color, surface brightness, environment, metallicity and stellar mass.

GALEX (Galaxy Evolution Explorer) is a NASA Small Explorer, launched in April 2003. We gratefully acknowledge NASA’s support for construction, operation, and science analysis for the GALEX mission, developed in cooperation with the Centre National d’Etudes Spatiales of France and the Korean Ministry of Science and Technology.

REFERENCES

- Abazajian, K. et al. 2003, *AJ*, 126, 2081
- Arnouts, S., et al. 2004, this volume
- Bell, E. F. 2002, *ApJ*, 577, 150
- Bertin, E., & Arnouts, S. 1996, *A&AS*, 117, 393
- Bruzual, G., & Charlot, S. 2003, *MNRAS*, 344, 1000
- Buat, V., et al. 2004, *ApJ*, this volume
- Cardelli, J. A., Clayton, G. C., & Mathis, J. S. 1989, *ApJ*, 345, 245
- Charlot, S., & Fall, S. M. 2000, *ApJ*, 539, 718
- Colless, M., et al. 2001, *MNRAS*, 328, 1039
- Cowie, L. L., Songaila, A., & Barger, A. J. 1999, *AJ*, 118, 603
- Davis, M., & Huchra, J. 1982, *ApJ*, 254, 437
- Felten, J. E. 1976, *ApJ*, 207, 700
- Gallego, J., Zamorano, J., Aragón-Salamanca, & Rego, M. 1995, *ApJ*, 455, L1
- Hawkins, E., et al. 2003, *MNRAS*, 346, 78
- Kennicutt, R. C. 1998, *ARA&A*, 36, 189
- Kong, X., Charlot, S., Brinchman, J., & Fall, S. M. 2004, *MNRAS*, 349, 769
- Kron, R. G. 1980, *ApJS*, 43, 305
- Lilly, S. J., Le Fèvre, O., Hammer, F., & Crampton, D. 1996, *ApJ*, 460, L1

- Martin, C. et al. 2004, ApJ, this volume
- Milliard, B., Donas, J., Laget, M., Armand, C. & Vuillemin, A., 1992, A&A, 257, 24
- Morissey, P. et al. 2004, ApJ, this volume
- Pérez-González, P. G., Zamorano, J., Gallego, J., Aragón-Salamanca, A., & Gil de Paz, A. 2003, ApJ, 591, 827
- Sandage, A., Tammann, G. A., & Yahil, A. 1979, ApJ, 232, 352
- Schechter, P. 1976, ApJ, 203, 297
- Schiminovich, D., et al. 2004, this volume
- Schlegel, D. J., Finkbeiner, D. P., & David, M. 1998, ApJ, 500, 525
- Somerville, R. S., Primack, J. R., & Faber, S. M. 2001, MNRAS, 320, 504
- Sullivan, M., Treyer, M. A., Ellis, R. S., Bridges, T. J. Milliard, B., & Donas, José 2000, MNRAS, 312, 442
- Treyer, M. A., Ellis, R. S., Milliard, B., Donas, J., Bridges, T. J. 1998, MNRAS, 300, 303
- Treyer, M. A., et al. 2004, this volume
- Wilson, G., Cowie, L. L., Barger, A. J., & Burke, D. J. 2002, AJ, 124, 1258
- Xu, C. K. et al. 2004, ApJ, this volume